applied sciences

MDPI

Article

Gait Recognition Algorithm of Coal Mine Personnel Based on LoRa

Yuqing Yin [1], Xuehan Zhang [1], Rixia Lan [1], Xiaoyu Sun [1], Keli Wang [1] and Tianbing Ma [2,*]

[1] School of Computer Science and Technology, China University of Mining and Technology, Xuzhou 221116, China; yinyuqing@cumt.edu.cn (Y.Y.); xuehanzhang@cumt.edu.cn (X.Z.); lan_rx@cumt.edu.cn (R.L.); 12203722@cumt.edu.cn (X.S.); 12205114@cumt.edu.cn (K.W.)

[2] State Key Laboratory of Mining Response and Disaster Prevention and Control in Deep Coal Mines, Anhui University of Science and Technology, Huainan 232000, China

* Correspondence: tbma@aust.edu.cn

Abstract: This study proposes a new approach to gait recognition using LoRa signals, taking into account the challenging conditions found in underground coal mines, such as low illumination, high temperature and humidity, high dust concentrations, and limited space. The aim is to address the limitations of existing gait recognition research, which relies on sensors or other wireless signals that are sensitive to environmental factors, costly to deploy, invasive, and require close sensing distances. The proposed method analyzes the received signal waveform and utilizes the amplitude data for gait recognition. To ensure data reliability, outlier removal and signal smoothing are performed using Hampel and S-G filters, respectively. Additionally, high-frequency noise is eliminated through the application of Butterworth filters. To enhance the discriminative power of gait features, the pre-processed data are reconstructed using an autoencoder, which effectively extracts the underlying gait behavior. The trained autoencoder generates encoder features that serve as the input matrix. The Softmax method is then employed to associate these features with individual identities, enabling LoRa-based single-target gait recognition. Experimental results demonstrate significant performance improvements. In indoor environments, the recognition accuracy for groups of 2 to 8 individuals ranges from 99.7% to 96.6%. Notably, in an underground coal mine where the target is located 20 m away from the transceiver, the recognition accuracy for eight individuals reaches 93.3%.

Keywords: LoRa; gait recognition; identification of underground personnel in coal mines; received signal amplitude; autoencoder

check for updates

Citation: Yin, Y.; Zhang, X.; Lan, R.; Sun, X.; Wang, K.; Ma, T. Gait Recognition Algorithm of Coal Mine Personnel Based on LoRa. *Appl. Sci.* **2023**, *13*, 7289. https://doi.org/10.3390/app13127289

Academic Editor: Byung-Gyu Kim

Received: 25 May 2023
Revised: 15 June 2023
Accepted: 16 June 2023
Published: 19 June 2023

Copyright: © 2023 by the authors. Licensee MDPI, Basel, Switzerland. This article is an open access article distributed under the terms and conditions of the Creative Commons Attribution (CC BY) license (https://creativecommons.org/licenses/by/4.0/).

1. Introduction

The coal mine underground personnel position monitoring system [1] is an integral component of safety hedge, aimed at tracking the location of underground workers. This system encompasses various functionalities, including the management and retrieval of entry and exit times for card-carrying personnel and access times to key and restricted areas. Of these functionalities, identity recognition plays a critical role in the system's operation. Fingerprint and face recognition technologies are commonly employed in underground coal mines for this purpose. However, the underground environment presents numerous challenges, such as high levels of coal dust, limited visibility, confined spaces, elevated temperatures, and high humidity. These factors adversely affect the clarity of fingerprints and faces, consequently impacting identification accuracy.

Human identity recognition typically relies on one or more internal physiological characteristics [2–4] (such as fingerprints, iris patterns, palm lines, and other external body features) or behavioral characteristics [5–7] (such as typing style, gait, voice rhythm, and other behavioral patterns). Among these, gait recognition is an emerging biometric technology that offers several advantages over fingerprint and face recognition, including non-invasiveness, long-range identification capability, minimal environmental influence,

and difficulty in disguising. Traditional gait recognition research often involves the use of cameras [8,9], acceleration sensors [10], and ground sensors [11] to capture movement information. However, these devices are susceptible to issues such as illumination variations, smoke interference, and physical obstacles, which significantly limit their effectiveness in harsh mining environments.

In recent years, there has been significant interest in human behavior sensing using wireless signals. This sensing technique is based on the principle that human activities impact the propagation of wireless signals, leading to distinct patterns of signal variations. By establishing the relationship between these signal variation patterns and human activities, it becomes possible to determine the state of human activity. This wireless-based approach offers several advantages over sensor-based gait recognition methods. It does not rely on optimal lighting conditions or the use of specialized sensor devices, making it particularly suitable for the challenging underground environment of coal mines characterized by low visibility, high levels of dust, and humidity. Currently, gait recognition achieved through the collection of WiFi Channel State Information (CSI) demonstrates high accuracy. However, its sensing range is limited, making it unsuitable for long-distance roadway applications in underground environments.

In order to address the aforementioned challenges, this research paper introduces the utilization of long-range radio (LoRa) signals for gait recognition, representing the first known application of LoRa signals in this context. In comparison to the wireless signals discussed earlier, LoRa signals offer distinct advantages, including extended propagation distance and enhanced penetration capabilities. These characteristics make LoRa signals particularly well-suited for long-distance wireless sensing in underground environments. The propagation range of LoRa signals can reach up to 10 km in rural areas and several kilometers in urban areas [12,13]. Furthermore, LoRa terminals are cost-effective, with prices ranging from USD 5 to 15 per unit. They also boast a battery life exceeding ten years, making them highly durable. LoRa technology has already been widely deployed in numerous Asian and European countries, adding to its feasibility and accessibility for practical implementation.

Gait recognition based on LoRa signals faces the following key challenges: (1) Gait recognition based on other wireless signals has achieved certain research results, but we adopt LoRa signals for gait recognition for the first time. Therefore, its feasibility needs to be further verified. (2) In the process of walking, the body shape and movement mode of the target will affect the propagation of wireless signals. How to extract appropriate features representing individual uniqueness to effectively recognize the target identity is also a challenge for the research of this paper.

This paper introduces a gait recognition system based on LoRa signals, designed to enable identity recognition in single target scenarios by analyzing the impact of different individuals on wireless signals. The proposed system offers simplicity in deployment, ease of operation, and practicality. To address the aforementioned challenges, the research focuses on comparing and analyzing the signal variation patterns caused by different individuals. The findings demonstrate that even individuals with similar height and weight exhibit distinct signal variation patterns due to their unique walking gaits. These results serve as an experimental foundation for gait recognition based on LoRa signals. In the feature extraction stage, an autoencoder is employed to automatically learn the features of data samples. The autoencoder is then combined with a Softmax layer to construct a deep learning network. The network is trained using the gradient descent method, enabling single-target identity recognition. By leveraging these approaches, the proposed gait recognition system based on LoRa signals offers promising potential for the accurate and efficient identification of individuals in real-world applications. The main contributions of this paper are as follows.

- This paper is the first work to apply the LoRa signal to gait recognition. We verify the feasibility of gait recognition based on LoRa signals and construct a gait recognition dataset. The gait recognition algorithm is studied by analyzing and processing the wireless signals received by the LoRa gateway.
- We analyze the signal change pattern when the target walks. Based on the amplitude data of the received signal, the features of the target when walking are extracted using an autoencoder. We transform it into a multi-classification problem to further identify the target identity.
- Many gait recognition experiments are carried out to compare the various impacts of the recognition accuracy. The results show that the recognition accuracy of 2~6 people in an indoor environment is 99.7~95.6%. In the coal mine underground environment, the recognition accuracy of six people can still reach 90.2% at a long distance of 20 m.

2. Materials and Methods

2.1. Wireless Sensing Model Based on LoRa

LoRa is a physical-layer technology for long-range, low-power wireless communication. LoRa encodes the data as chirps whose frequencies vary linearly over time by the chirp spread spectrum (CSS) modulation technique [14]. The complex exponential representation of a linear frequency modulation (LFM) [15] chirp can be represented as:

$$T_x(t) = e^{(j2\pi f_c t + j\pi k t^2)} = \cos\left(2\pi f_c t + \pi k t^2\right) + j \cdot sin\left(2\pi f_c t + \pi k t^2\right), \quad (1)$$

where f_c is the central frequency, $k = B/T$ is the sweep rate of the chirp, B is the bandwidth, and T is the sweep time. The in-phase (I) and quadrature (Q) components of the LFM chirp can be represented as:

$$I(t) = \cos(\phi(t)) = \cos\left(2\pi f_c t + \pi k t^2\right), \quad (2)$$

$$Q(t) = \sin(\phi(t)) = \sin\left(2\pi f_c t + \pi k t^2\right), \quad (3)$$

where $\phi(t)$ is the instantaneous phase. The instantaneous frequency is a linear function of time, which can be calculated as $\frac{1}{2\pi}\frac{d(\phi(t))}{dt} = kt + f_c$. Figure 1 shows the frequency domain and time domain waveforms of an LFM signal. Through the time of one cycle ($-T/2 \le t \le T/2$), the frequency varies linearly from $f_c - B/2$ to $f_c + B/2$. As shown in Figure 1b, the corresponding time domain signal is a cosine wave with increasing frequency over time. Due to the full utilization of the whole allocated bandwidth for encoding data, the chirp is more robust against channel noise and multipath and Doppler effects.

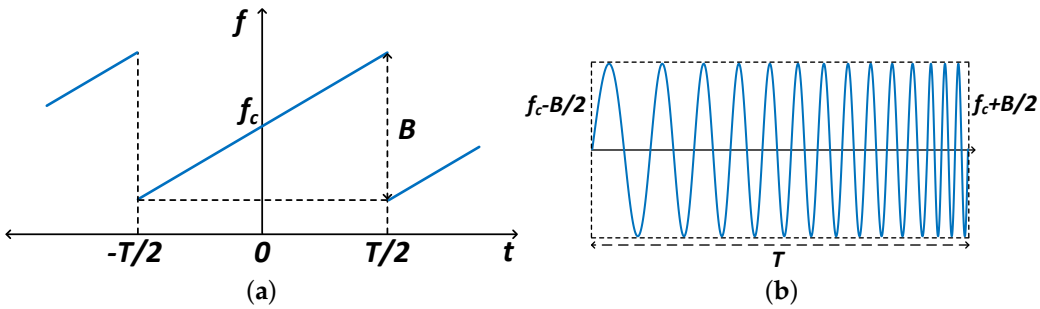

Figure 1. Waveform of a chirp signal. (**a**) Frequency domain signal representation. (**b**) Time domain signal representation.

As shown in Figure 2, the LoRa signal can be reflected by static objects (such as walls and rocks) and dynamic objects (such as human targets) in the propagation process from a transmitter node to a receiver gateway. Supposing that the signal reaches the receiver through N different paths, the received signal can be represented as:

$$R_x(t) = e^{j(\pi k t^2 + \theta_c + \theta_s)} \sum_{n-1}^{N} a_n(t) e^{-j2\pi f_c \tau_n(t)}, \tag{4}$$

where $\theta_c = 2\pi\Delta f t$ ($\Delta f = f_c - f_c^{'}$) is the carrier frequency offset (CFO) caused by unsynchronized clocks between the transmitter and receiver, θ_s is the sampling frequency offset (SFO), $a_n(t)$ is the composite representation of the attenuation factor and initial phase of the nth path, and $\tau_n(t)$ is the time delay of the nth path.

The N multipaths can be further divided into static and dynamic paths. The static paths include the direct and reflection paths of static objects such as the walls and ground. The dynamic paths include the reflection paths of the moving targets. The static and dynamic vectors in the I-Q vector space are shown in Figure 3. The signal vector length represents the amplitude, and the angle with the I-axis represents the phase. The sum of the static and dynamic vectors is the composite vector, which can be directly extracted from the receiver. When the target is moving, the static vector is unchanged because the static objects keep their original states. Meanwhile, the target movement causes a change in the dynamic path length, and the dynamic vector rotates around the static vector.

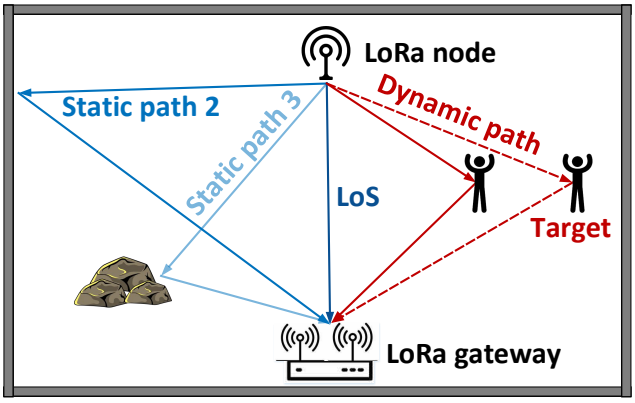

Figure 2. Sensing scenario.

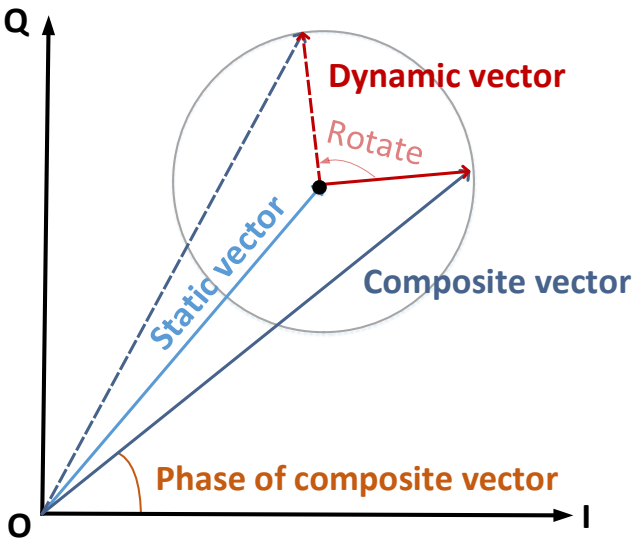

Figure 3. Signal vector representation.

2.2. Preliminary Experiment

For gait recognition based on LoRa signals, the first challenge we faced was whether the target's walking would induce obvious variation patterns and whether different targets walking under the same experimental conditions would cause different signal variation patterns. To verify the feasibility of gait recognition based on LoRa signals, we designed a preliminary experiment.

The experiment scenario was a laboratory environment covered with desks, chairs, and computers on both sides, where the multipath effect was significant. The transmitter and receiver were placed side by side. The target was located at a distance of 5 m from the transceiver and walked perpendicular to the line of sight (LOS) for a total of four round trips. The experiment results are shown in Figure 4. The top and bottom figures represent the normalized amplitudes of the received signals for users A and B, respectively. We observed that the four round trips of the user's walking corresponded to the four variation periods of the received signal, indicating that the LoRa-received signals contained the walking information of the target. In addition, the received signals for different targets show similar periodicity when they carried out the same walking process. However, the signal variation patterns in the same period were obviously different, and the corresponding period lengths were also different. A longer period represented a slower target walking speed, whereas a shorter period indicated a faster target walking speed.

In the same place, the gait of the same target walking over time was reflected in the consistency of the received signal, which determined whether the same target could be recognized at different times in the same place. In the process of data collection, the target was required to repeat the walking process. It was observed that the received signal variations caused by the target walking remained basically consistent over an hour. The above preliminary experiment and analysis verified the difference between different target gaits and the consistency of the same target gaits over time, which provides an experiment basis for LoRa-based gait recognition research and proves the feasibility of gait recognition by processing LoRa received signals.

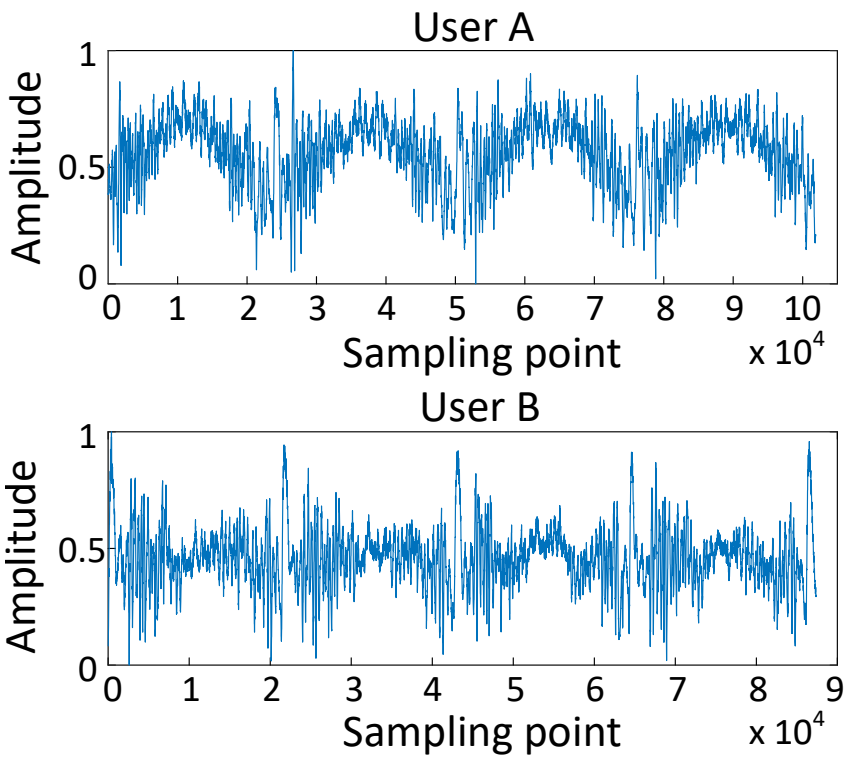

Figure 4. Amplitude of received signal.

2.3. System Architecture

As shown in Figure 5, the proposed system consists of three modules: data collection, data preprocessing, and feature extraction and identity recognition.

Data collection: In the process of data collection, a pair of LoRa transceivers was deployed. The LoRa node continuously transmits wireless signals, and the target walks in the sensing area. The LoRa gateway receives signals reflected by the direct path, the surrounding environment, and the moving target. By analyzing the received signals, we can obtain the target movement information.

Data preprocessing: In the propagation process, signals are interfered with by other noises. Before the feature extraction of the received signals, it was necessary to select an appropriate filter for noise reduction of the received signals. In order to transform the received signal amplitudes in the dimensionless form for calculation and comparison, we normalized the amplitudes. According to the preliminary experiment, the received signals showed periodic variations during the round-trip walking of the target, and different targets showed different waveform characteristics. In this paper, the target walking period was determined based on the autocorrelation method, and the signals were divided to construct the training set and the test set according to the waveform periodicity.

Feature extraction and identity recognition: In the feature extraction stage, the autoencoder was trained to effectively reconstruct the preprocessed data so that it could extract the effective features of the gait behavior. The encoder in the trained autoencoder was stacked with the Softmax layer to generate a deep learning network, which output the individual identity corresponding to the gait behavior and realized single-target gait recognition based on LoRa.

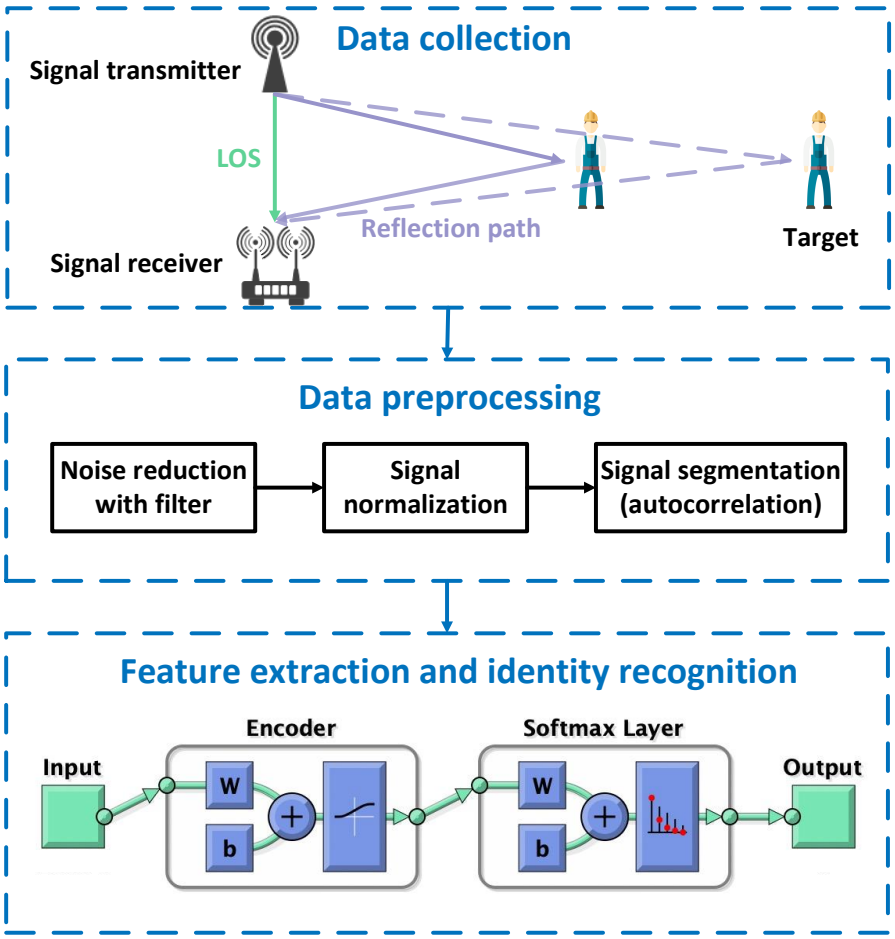

Figure 5. System architecture.

2.4. Data Preprocessing

In this paper, we first used the Hampel algorithm to remove outliers from the original signal. For each sample of the input signal vector, the Hampel function calculates the median of a window consisting of that sample and the surrounding 2000 samples, 1000 on each side. After that, we used the absolute value of the median to estimate the standard deviation of each sample to the median, and if the standard deviation of the sample from the median exceeded three standard deviations, we replaced the sample with median to replace that sample. After removing the outliers from the original signal, the signal was smoothed using S-G (Savitzky–Golay) filtering and the high-frequency noise was removed using a Butterworth filter. Through experiments, we found that when human targets are walking, the main movement is from the legs and arms, whose frequency is usually 1.7–10 Hz. Therefore, we adopt Butterworth filter with cutoff frequency of 1.7–10 Hz. The signals before and after filtering are shown in Figure 6.

2.5. Signal Segmentation Based on Autocorrelation

When the human body walks back and forth perpendicular to the LOS path, the received signal presents regular periodicity. We used the autocorrelation algorithm to calculate the period of the signal so that we could segment the signal to construct the training and test sets.

Autocorrelation, also known as sequence correlation, is the cross-correlation between a signal and itself at different points in time. Autocorrelation can find periodic signals masked by noise and is often used in time domain signal analysis. Its mathematical definition is as follows:

$$R_{xx}(\tau) = \int_{-\infty}^{+\infty} x(t)x(t+\tau)dt, \tag{5}$$

where τ is the step length in comparison. $x(t)$ is time-shifted to obtain $x(t+\tau)$, and multiplied by $x(t+\tau)$ point-by-point over the whole range to produce a curve; the area under the curve is the value R. By changing τ and repeating the process, an autocorrelation curve $R(\tau)$ could be drawn. As shown in the above Figure 7, the period span of the target movement was 27,425 samples. The signals were divided based on this period, and the segmentation results are shown in Figure 7.

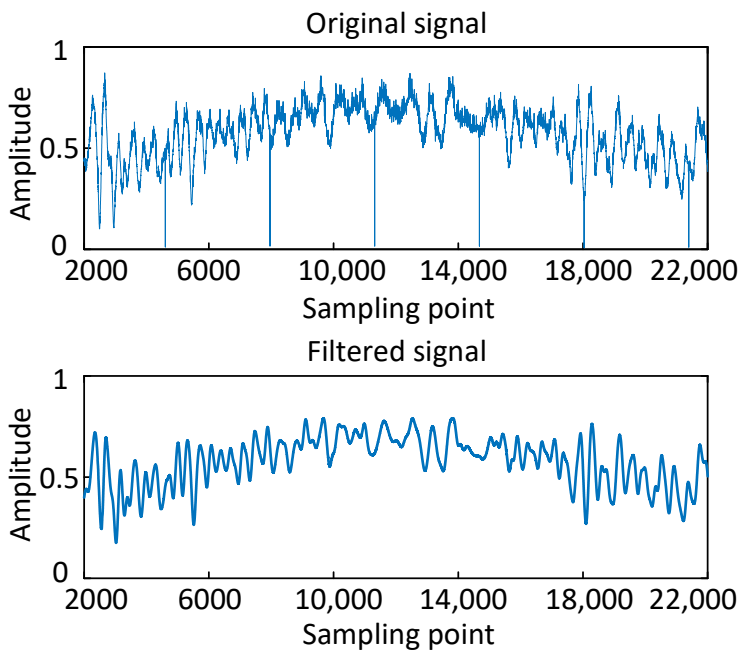

Figure 6. Signal amplitude before and after filtering.

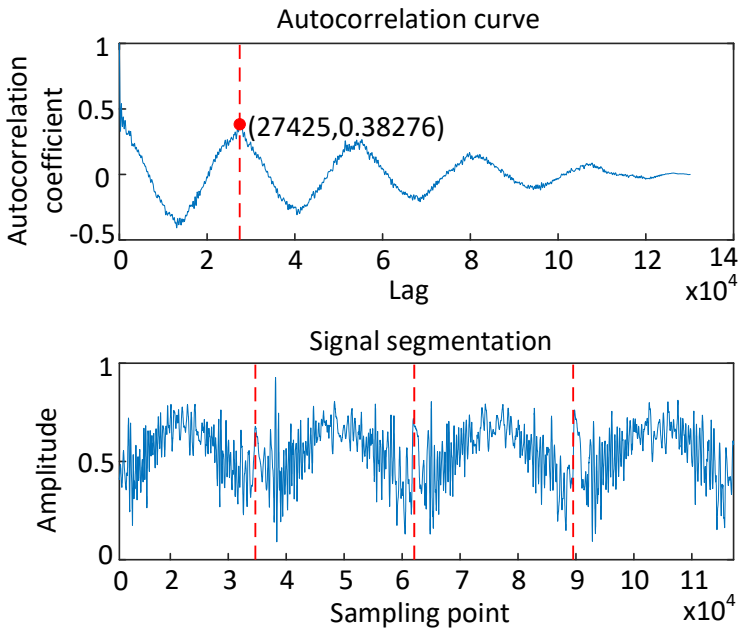

Figure 7. Signal segmentation.

2.6. Feature Extraction and Identity Recognition

2.6.1. Feature Extraction Based on Autoencoder

The experiment results show that different human targets have unique signal variation patterns when walking. Based on the analysis of the received signal waveform, the autoencoder was used as the feature extractor to effectively reconstruct the preprocessed data and extract the effective features of individual gait behavior to further input the learned features into the supervised model and identify the target identity.

Autoencoders, first proposed by Rumelhart, Hinton, and Williams in 1986, aim to learn the information representation of data in an unsupervised manner and reconstruct its input after training. The encoder A $\mathbb{R}^p \rightarrow \mathbb{R}^n$ and the decoder B $\mathbb{R}^n \rightarrow \mathbb{R}^p$ satisfy the following equation:

$$\text{argmin}_{A,B}\, B^{E[\Delta(x,B^{\circ}A(x))]}, \tag{6}$$

where E is the expectations of the x distribution, and Δ is the reconstructed loss function for calculating the distance between the decoder output and input. The latter is usually set to the l_2 norm.

The autoencoder is mainly composed of the encoder and decoder, as shown in the green part of Figure 8. It is a neural network with the same structure of the input and output vectors. The encoder compresses the high-dimensional input code into low-dimensional hidden variables from which it extracts features that can represent the input data. The encoder compresses the high-dimensional input code into low-dimensional hidden variables from which it extracts features that can represent the input data. The decoder restores the hidden variable to its original dimension, and its output approximately restores the original input. In the training process, the autoencoder extracts the gait features of different human targets during walking, which represent the original input signals to the greatest extent and can effectively distinguish different targets to achieve target identification.

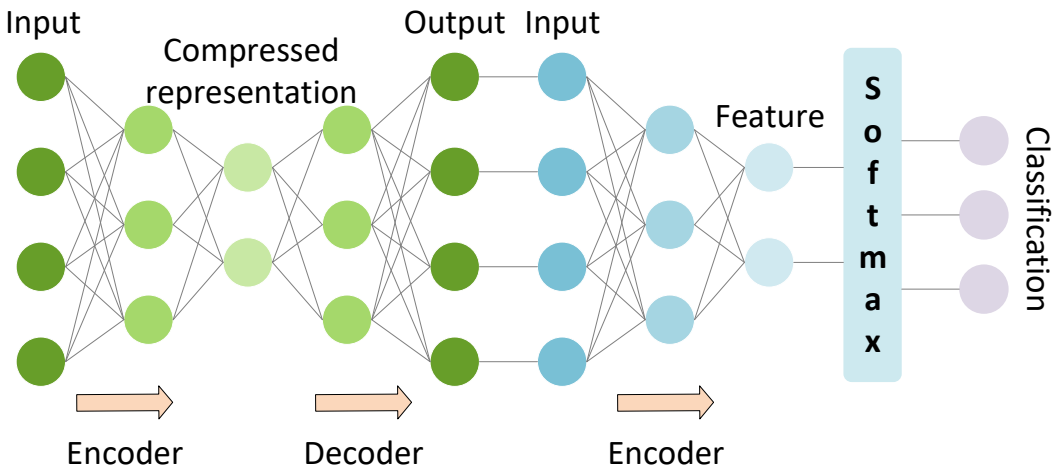

Figure 8. Network model.

2.6.2. Identity Recognition Based on Softmax

Softmax function, also known as the exponential normalization function, is a normalized form of Logistic function, which is often used to deal with multiple classification problems. In this paper, the features generated by the encoder in the trained encoder are taken as the input matrix, which is classified by the Softmax method, and the individual identity corresponding to the gait behavior is output. The network model is shown in Figure 8.

In Softmax regression, for each input x, its corresponding output y is a vector of length K. When class c is the correct class, we let $y_c = 1$ and the other elements of the y vector be 0, i.e., one-hot vector ($y_c = 1$ and $y_j = 0, \forall j \neq c$). The classifier finally outputs an estimate vector $\hat{y}$. For each class k, the value of $\hat{y}_k$ is the estimate of probability $p(y_k = 1 \mid x)$.

For vector z with dimension K, Softmax is defined as:

$$\mathrm{Softmax}(z_j) = \frac{\exp(z_j)}{\sum_{j=1}^{K} \exp(z_j)}, 1 \leq i \leq K. \tag{7}$$

After the input vector z passes Softmax, the vector is obtained:

$$\mathrm{Softmax}(z) = \left[\frac{\exp(z_1)}{\sum_{i=1}^{K} \exp(z_i)}, \frac{\exp(z_2)}{\sum_{i=1}^{K} \exp(z_i)}, \cdots, \frac{\exp(z_K)}{\sum_{i=1}^{K} \exp(z_i)} \right]. \tag{8}$$

The sum of all elements in this vector is 1, and the denominator $\sum_{i=1}^{K} \exp(z_i)$ is used to normalize all the values into probabilities.

3. Results

We first implemented a prototype gait recognition system based on LoRa in an indoor environment, and explored the effects of different numbers of people, different sample sizes, and wall penetration on recognition accuracy. Moreover, in order to verify the applicability of the prototype system in an underground coal mine environment, long-distance gait recognition experiments were carried out in an underground coal mine roadway. At the end, the classification performance of different models was explored for indoor, underground, and through-wall environments.

3.1. Experiment Setup

Front-end hardware: As shown in Figure 9, the prototype system proposed in this paper consists of a pair of LoRa transceivers. The LoRa transmitter consists of Arduino Uno and Semtech SX1276 modules and is equipped with an antenna. LoRa nodes transmit signals in the 915 MHz band with a 125 kHz channel bandwidth and transmit power of 20 dBm. The receiver is a USRP X310, receiving signals at a sampling rate of 1 kHz and equipped with two antennas. The LoRa transceiver is equipped with three-directional antennas with a gain of 8 dbi.

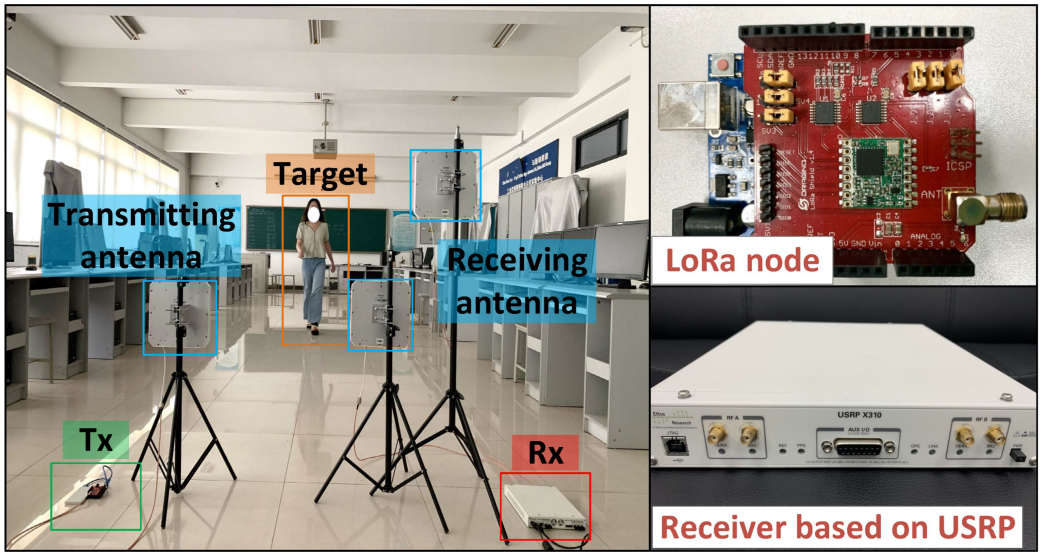

Figure 9. Experiment scenario deployment diagram.

Back-end implementation: The USRP X310 was connected to a Lenovo ideapad 700 laptop with an Intel Core i5-6300HQ CPU and 8.0 GB RAM via a network cable. We used Labview software to collect LoRa signals, and MATLAB was used to process the collected signals.

Experiment environment: As shown in Figure 9, we conducted the evaluation experiment in a laboratory environment with a length of 12 m and a width of 6.5 m. The distance between the LoRa transceiver devices was 1 m, and the height of the transmitting antenna was set to 0.8 m. The height of receiving antenna 1 was set to 0.8 m, and the height of receiving antenna 2 was set to 1.3 m. The target travelled back and forth in the LOS direction perpendicular to the position 5 m away from the transceiver.

3.2. Indoor Laboratory Environment

3.2.1. Experiment Result

The above method was used to collect 2560 sets of data from eight users (five males and three females), of which 75% (1920 sets of data) was used as the training set and the remaining 25% (640 sets of data) was used as the test set. The experimental results are shown in the confusion matrix in Figure 10, where the columns represent the real identity of the user and the rows represent the identity predicted by the classifier. In the laboratory scenario, the recognition accuracy of eight users was 96.6%, which verifies the feasibility of gait recognition based on LoRa signals and lays a foundation for the application of user gait recognition in the future.

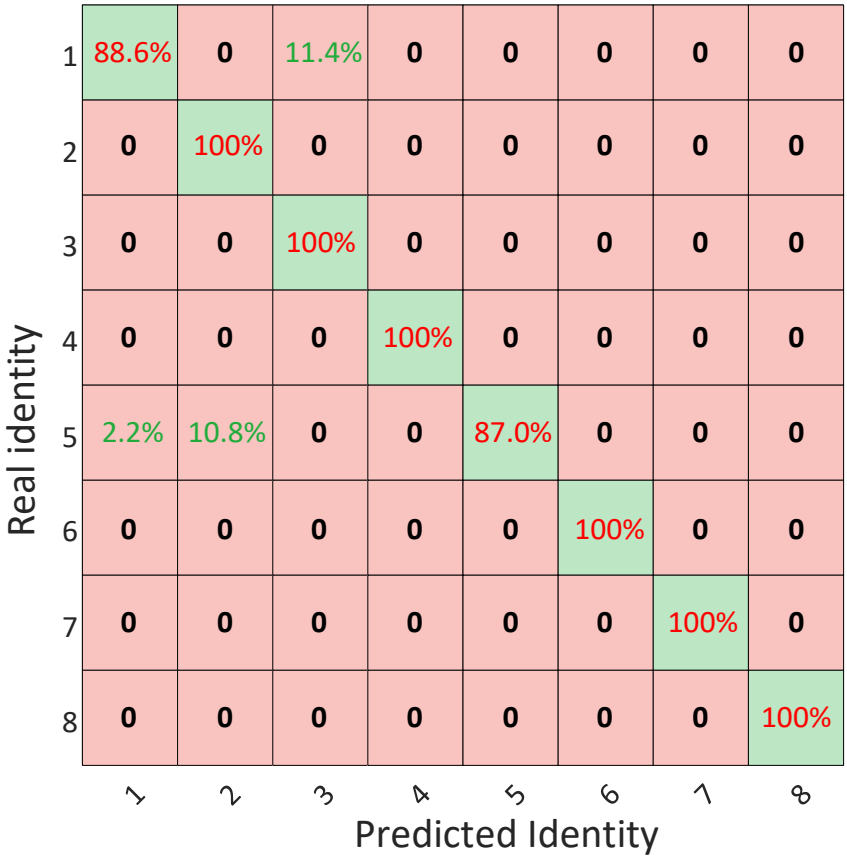

Figure 10. Confusion matrix of experiment.

3.2.2. Recognition Accuracy for Different Numbers of People

Figure 11 shows the recognition accuracy for different numbers of people in the laboratory scenario. When the people number of recognition increased from two to eight, the corresponding recognition accuracy was 99.7~96.6%. With the increased number of users, the recognition accuracy gradually decreased. This is because when the number of users increases, the size and walking pattern of some users may be similar and difficult to distinguish, which leads to a decrease in the recognition accuracy.

3.2.3. Recognition Accuracy of Different Sample Sizes

In order to determine the impact of training sample size on classification performance, we tested the recognition accuracy of training sets of different sizes. The experiment results are shown in Figure 12, and the abscissa represents the subsampling interval. When the interval was 1, the sample size was 1920 sets of data, and when the interval was 6, the sample size was 320 sets of data. As shown in the figure, when the training sample size decreased from 1920 sets of data to 320 sets of data, the recognition accuracy decreased from 96.6% to 91.1% under the same network model parameters. Under normal circumstances, when the sample interval increased, the training sample size decreased and the recognition accuracy decreased. Since the quality of the samples was high, the recognition accuracies were similar when the sample interval was large, such as 5 or 4. However, when the sample interval increased, the overall trend of the recognition accuracy was decreasing. Therefore, the default training sample size in the experiment was set to 1920 sets of data.

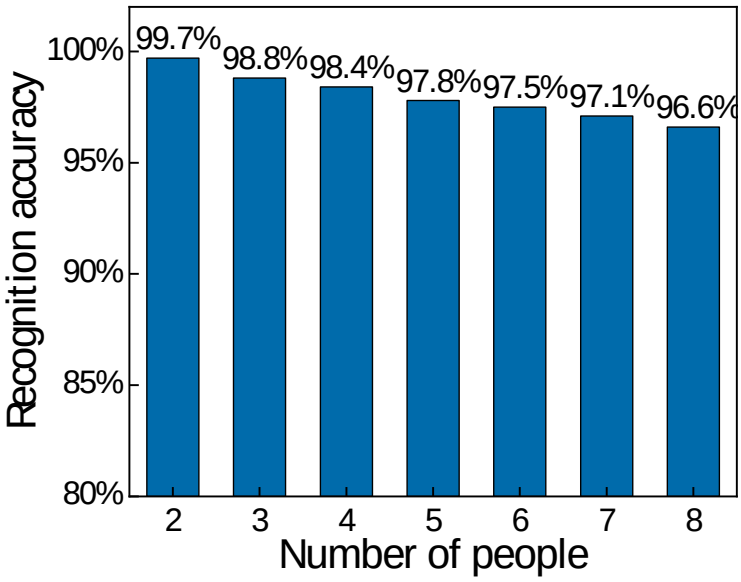

Figure 11. Recognition accuracy of a different number of people.

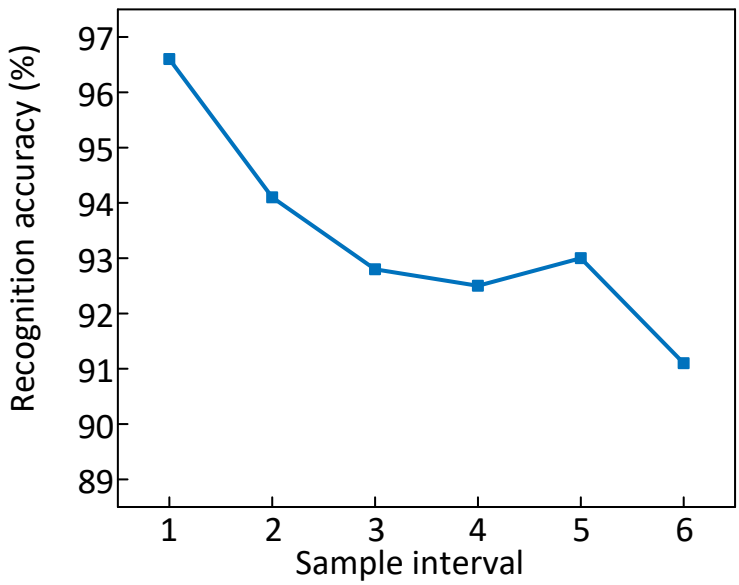

Figure 12. Recognition accuracy of different sample sizes.

3.2.4. Impact of Through-Wall Sensing

We explore the impact of through-wall gait recognition in the meeting room. The experiment scenario is shown in Figure 13. The transceiver was located on one side of the wall, which was a 17 cm thick concrete wall. The target was located 5 m away from the wall on the other side. The experiment results are shown in Figure 14. In the case of 2~8 people, the recognition accuracy was 99.9~95.6%. Compared to line-of-sight-based lab scenes, the recognition accuracy decreased by only 1%. It shows that the system still has strong robustness in the scenario of penetrating the wall.

3.3. Coal Mine Underground Environment

3.3.1. Experiment Results

In order to verify the applicability of underground gait recognition systems based on LoRa, we conducted experiments in an underground coal mine environment similar to an indoor environment. The experiment schematic and scenario are shown in Figures 15 and 16. The experiment environment was a coal mine roadway, where the LoRa node and gateway

were placed side-by-side on one side of the roadway, and the target walked perpendicular to LOS at a position 5 m away from the transceiver. The experiment results are shown in Figure 17. For the eight-person scenario, the recognition accuracy was 93.8%.

Under the same experiment setting conditions, compared with the indoor environment, the recognition accuracy in the coal mine underground environment was slightly lower than in the indoor environment. This is because the environment in the coal mine underground environment is harsh, with high temperature, high humidity, and high dust concentration, which is not conducive to wireless signal transmission. Therefore, the human behavior perception performance based on a wireless signal is slightly lower than that in the indoor environment.

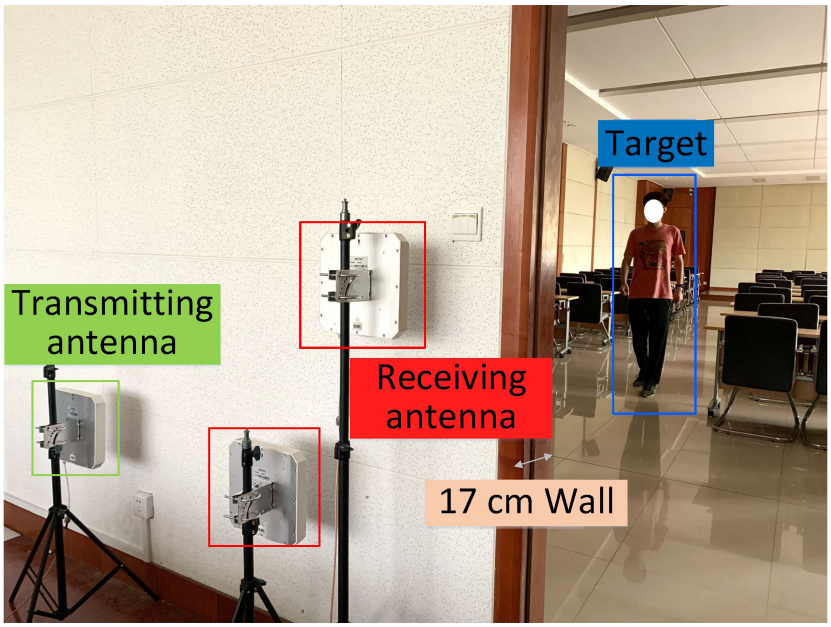

Figure 13. Scenario of through-wall experiments.

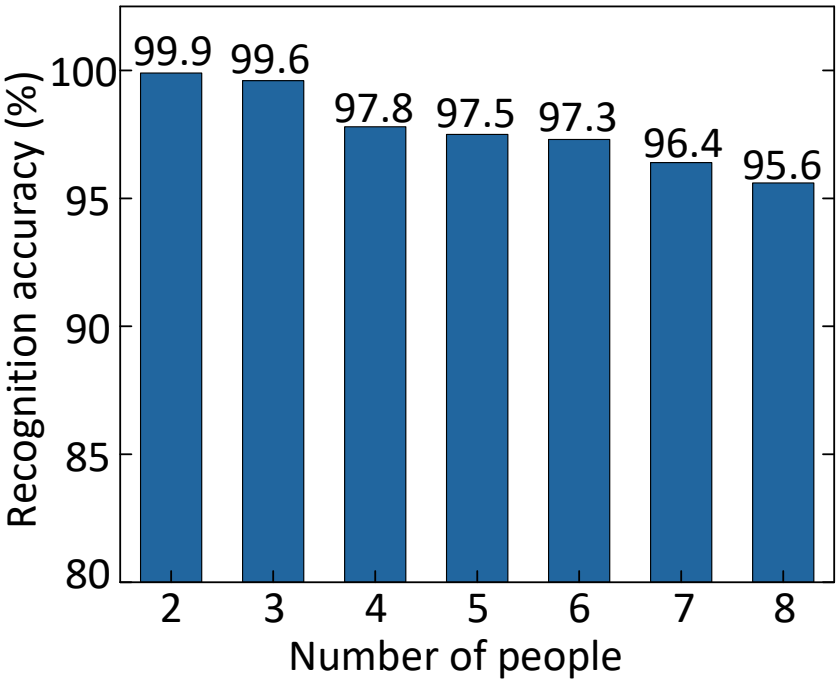

Figure 14. Recognition accuracy of different number of people in through-wall scenario.

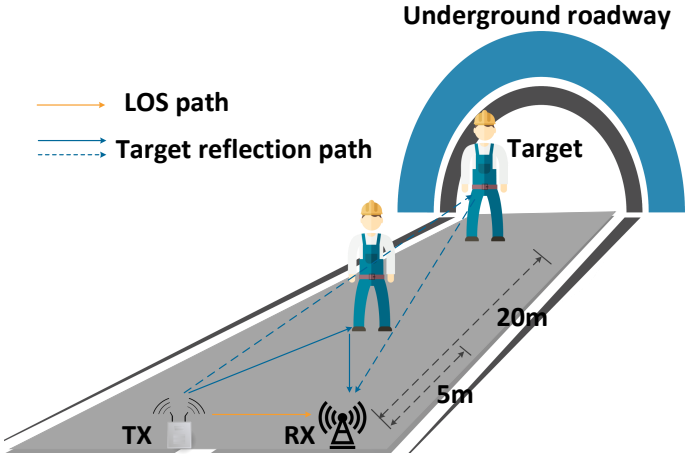

Figure 15. Diagram of coal mine underground.

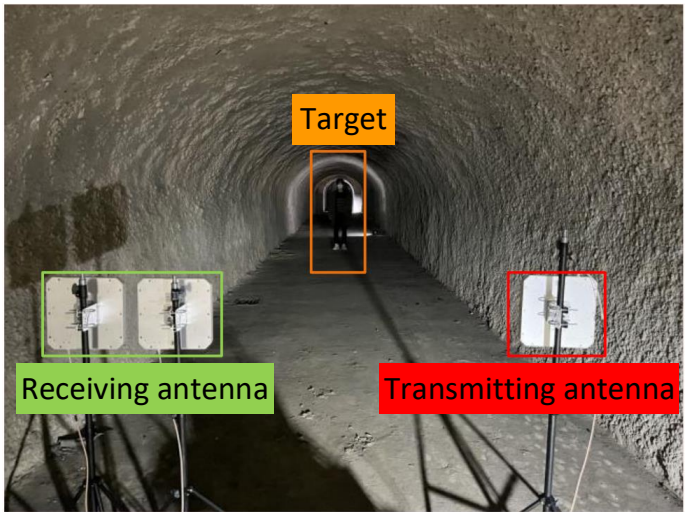

Figure 16. Scenario of coal mine underground.

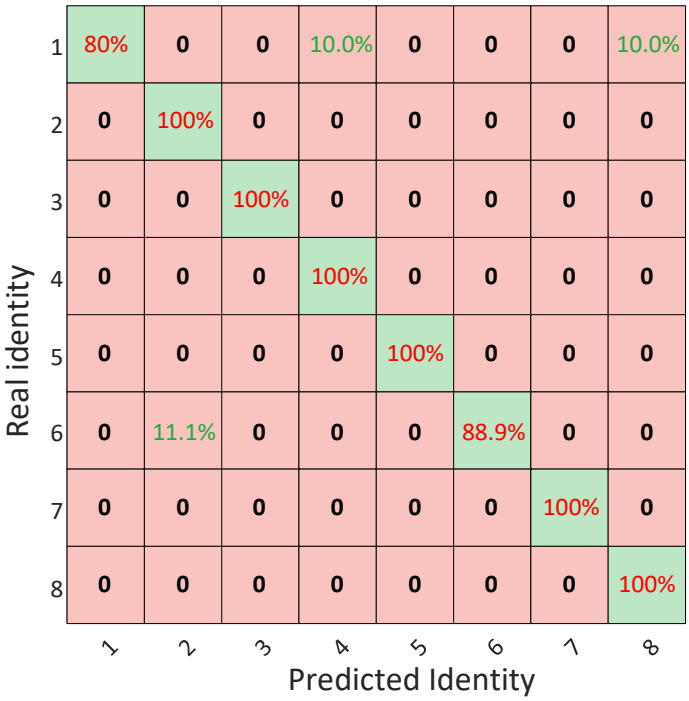

Figure 17. Confusion matrix with distance of 5 m.

3.3.2. Underground Long-Distance Sensing

We also verify the gait recognition performance under long-distance conditions in the coal mine underground environment. The experiment schematic diagram is shown in Figure 15. The target was perpendicular to LOS when it was 20 m away from the transceiver. Figure 18 shows the confusion matrix of experiment results. It can be seen from the figure that even if the target is 20 m away from the transceiver, the recognition accuracy only decreases by 0.5% compared with that of 5 m. The target identity can still be recognized effectively, which lays the foundation for long-distance gait recognition application. It is proved that the gait recognition system based on LoRa is feasible for long-distance sensing in the underground coal mine roadway.

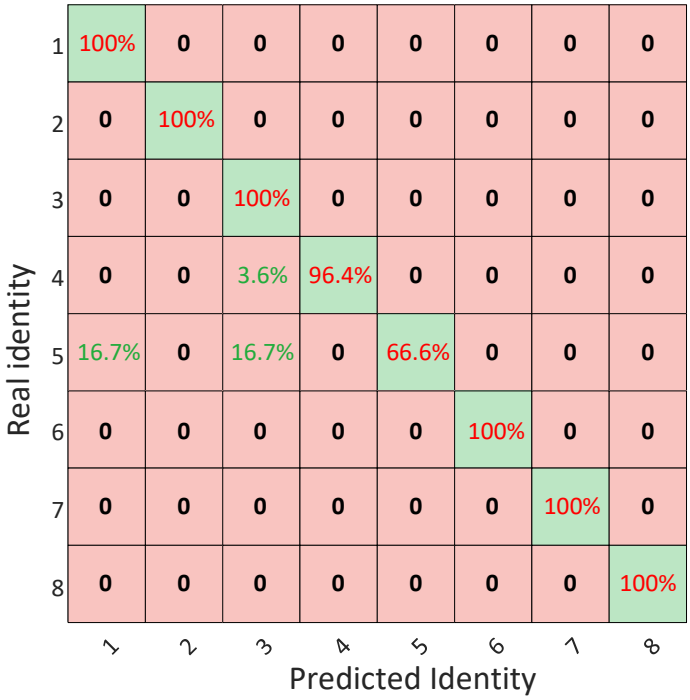

Figure 18. Confusion matrix with distance of 20 m.

3.4. Evaluation of Different Models

For the laboratory, coal mine underground, and through-wall scenarios, we adopted the autoencoder Softmax stacked network model, pattern recognition neural network (Patternnet), and K-nearest neighbor (KNN) to conduct experiments, respectively. Six people were employed in the laboratory and coal mine underground environment, and four people were employed in the through-wall environment. The results are shown in Figure 19. In the laboratory environment, the recognition accuracy of the model adopted in this paper was 1.3% and 2.9% higher than that of the Patternnet and KNN models, respectively. In the coal mine underground and through-wall environment, the recognition accuracy was 8.4% and 12.8%, and 7% and 6.3% higher than that of the Patternnet and KNN models, respectively. It can be seen from the above results that under the three experiment scenarios, the recognition accuracy of the network model adopted in this paper was superior to that of the Patternnet and KNN models, which can extract the gait features of signals more effectively, thus improving the recognition accuracy.

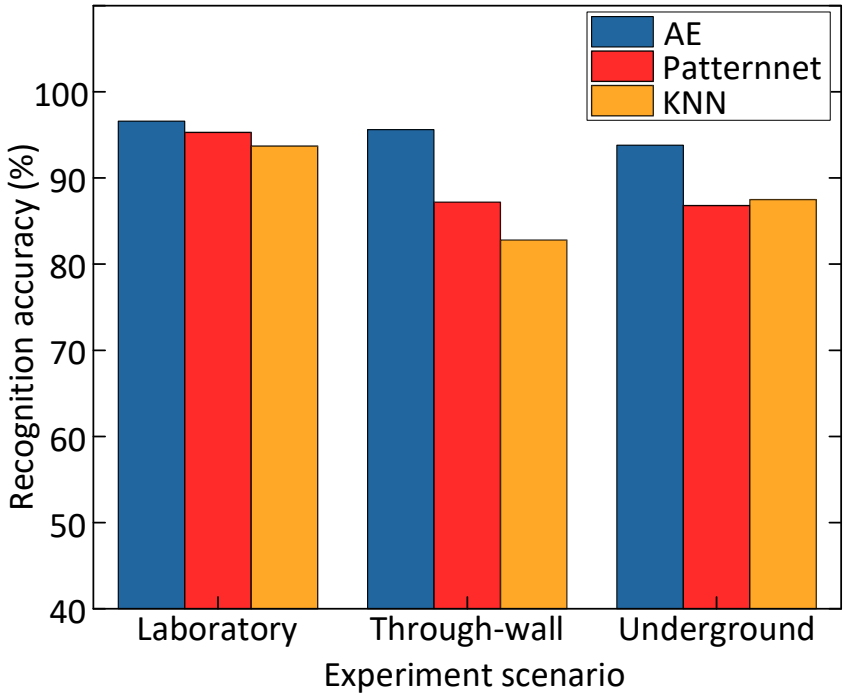

Figure 19. Comparison of recognition accuracy of different models.

4. Discussion

4.1. Related Work

4.1.1. Gait Recognition Based on Sensor

In traditional research based on gait recognition, sensors are often used to obtain movement information. Zhu et al. [16] proposed a real-time motion-tracking system based on tri-axis microelectromechanical accelerometers, rate gyros, and magnetometers by the Kalman algorithm. The results showed that the standard deviation of the heading angle was about 1.5°, and validated the effectiveness of the proposed method. Glowinski et al. [17] proposed a human gait analysis method by using a wavelet transform of the signal obtained from six inertial ProMove mini sensors. Tadano et al. [18] proposed a method for three-dimensional gait analysis using wearable sensors and quaternion calculations. The results showed that the average RMSE and correlation coefficient (CC) were 10.14 deg and 0.98, 7.88 deg and 0.97, 9.75 deg and 0.78 for the hip, knee and ankle flexion angles, respectively. However, these devices are susceptible to smoke and obstacles, and have great limitations in the harsh mine environment.

4.1.2. Gait Recognition for Coal Mine

The existing works on gait recognition in coal mines mainly use neural networks to process image data. Liu et al. [19] proposed a gait recognition method via similarity learning named two-stream neural network (TS-Net) based on a densely connected convolution network (DenseNet) and stacked convolutional autoencoder (SCAE). The experimental results show that the proposed TS-Net model has a gait recognition accuracy of 92.22% in the UCMP-GAIT dataset. Chao et al. [20] proposed a gait recognition method by combining wavelet packet transforms (WPT) and principle component analysis (PCA). Gait recognition results on the CASIA-A database showed the highest accuracy of 97.16% using WPT and PCA. Li et al. [21] proposed an improved YOLOv4 network for personnel detection based on thermal infrared images. Experimental results show that on the infrared personnel image dataset underground coal mine, the improved YOLOv4 model achieves 96.25% and 48.2 fps in global AP and detection speed, respectively. These image-based works are heavily affected by illumination.

4.1.3. Gait Recognition Based on Wireless Signal

With the popularity of WiFi devices, wireless sensing based on WiFi signals has made some achievements in the field of gait recognition due to its advantages of non-contact, easy deployment, non-invasive and unaffected by lighting conditions. Shi et al. [22] proposed a user authentication scheme based on deep learning by analyzing the disturbance characteristics of human daily activities on WiFi signal CSI data, and identified 11 targets in walking and stationary states with an accuracy of 94% and 91%, respectively. Wang et al. [23] proposed the WiFiU method to extract principal components from CSI through principal component analysis (PCA). Short-time Fourier transform (STFT) was used to convert PCA components into spectral graphs, from which gait features were extracted. The support vector machine (SVM) algorithm was used for matching to realize identity recognition, with the highest accuracy of 93.5%. Zeng et al. [24] proposed the WiWho method to pre-process signals through long-distance multipath elimination and Butterworth bandpass filter. After extracting gait features from CSI, the decision tree algorithm was used for identity recognition. A 92~80% accuracy was achieved in the scenario of 2~6 people. Zhang et al. [25] proposed the WiFi-ID method to calculate the time-domain and frequency-domain features of CSI data by using the ReliefF feature extraction algorithm. The sparse approximation-based classification (SAC) algorithm was used to identify the target, and the accuracy was 93~77% in the case of 2~6 people. Xin et al. [26] proposed the FreeSence method,combined with principal component analysis (PCA), discrete wavelet transform (DWT) and dynamic time warping (DTW) algorithm; CSI data were processed. In the case of 2~6 people, the recognition accuracy rate was 94.5~88.9%.

In recent years, millimeter wave radar technology has made good progress in the field of gait recognition because of its high bandwidth, accurate spatial resolution, and strong robustness to the environment. Vandersmissen et al. [27] used CNN to extract micro-Doppler (MD) gait features to realize gait recognition. In the scenario of five people, the classification error rate of this method on the verification set was 24.70%. The classification error rate on the test set was 21.54%. Zhao et al. [28] proposed the mID method, which is based on a millimeter wave radar point cloud for gait recognition for the first time. LSTM was used to extract the time series features of gait point cloud data, and the recognition accuracy rate reached 89% in the scenario of 12 people. Meng et al. [29] established the first publicly available millimeter wave radar gait point cloud dataset MmGait, and proposed the MmGaitNet method. The method could achieve 90% accuracy in single-person recognition, but the pedestrian path was a fixed path, and the method only achieved 45% accuracy in a random path. Li et al. [30] proposed the MTPGait method, constructed and released a millimeter wave radar 3D point cloud data set, and designed a neural network based on CNN+LSTM to extract the multi-scale spatio-temporal characteristics of the 3D point cloud in the spatial and temporal dimensions. The results show that under the single scene with any path, MTPGait is able to achieve a recognition accuracy rate of 96.7%, and 90.2% when two people coexist.

4.1.4. Wireless Sensing Based on LoRa

In previous work, human behavior perception based on LoRa mainly utilizes its long-distance communication capability. Hossain et al. [31] used LoRaWAN to transmit human activity data monitored by acceleration sensors, classified the four activities of staying, standing, walking, and running by extracting characteristic values, and further explored the relationship between data packet loss rate and recognition accuracy. The LoRaMote [32] system fixed the armband equipped with body temperature and pressure transducers on the human arm, and took advantage of the LoRaWAN long-distance transmission to transmit sensor data to the monitoring base station to remotely monitor the health status of the human target. Ke et al. [33] deployed LoRa nodes on Windows, corridors, and rooftops of university campuses, forming a mesh network to transmit data collected by sensors for monitoring campus activities.

In recent years, researchers conducted non-contact human behavior perception based on the LoRa signal itself. The Widesee [34] system utilizes the mobility of an unmanned aerial vehicle (UAV) and carries a pair of LoRa transceivers to detect and locate human targets in high-rise buildings. The Widesee prototype system has a broad application prospect in the field of disaster rescue. Zhang et al. [35] built a relationship model between human movement and LoRa signal changes, and verified its feasibility in the field of coarse and fine-grained behavior perception. The system can sense breathing when the target is 25 m away from the LoRa equipment or 15 m away from the wall, and track the walking distance and direction of the human body when it is 30 m away. However, this approach is limited to a single target scenario. Recently, the team [36] proposed using beamforming to simultaneously monitor the respiratory rates of five human targets, achieving an average accuracy of 98.1%. Xie et al. [37] proposed the concept of a virtual fence to reduce the interference of LoRa signals in the process of long-distance transmission and realize multi-target perception. However, this method needs to know the direction information of targets, which hinders its application in real scenes.

4.2. Proposed System and Future Work

The system proposed in this paper has the following deficiencies: First, the user must follow a predetermined path, which is only suitable for small spaces, such as narrow entrances or laneways. The recognition of free path gait is a very challenging problem for future research. Secondly, when there are multiple targets walking at the same time, it is difficult to separate the gait of multiple targets from the received signals. In the future, it is planned to use multiple devices to separate the gait signals from each user to achieve multi-target gait recognition.

5. Conclusions

Aiming at the problems of existing gait recognition methods, such as high cost, easily affected by the environment, close sensing distance, and invasibility, this paper proposes a gait recognition system based on LoRa signals for the first time. Based on the amplitude of the received signal, Hampel, S-G filter, and Butterworth filter are used for preprocessing. After that, the autoencoder is used to automatically learn the features of the data samples, and it is stacked with a Softmax layer to generate a deep learning network. The gradient descent method is used for training, so as to recognize the target identity. In the case of 2~6 people, the recognition accuracy reached 99.7~95.6%. In the coal mine, even if the target is 20 m away from the transceiver, the recognition accuracy rate can reach 90.2%, which verifies the effectiveness of long-distance gait recognition based on LoRa and its applicability in the coal mine environment.

Author Contributions: Conceptualization, X.Z.; data curation, R.L.; formal analysis, K.W.; funding acquisition, T.M.; investigation, X.S.; methodology, Y.Y. and R.L.; project administration, Y.Y.; resources, Y.Y.; software, X.S.; supervision, T.M.; validation, K.W.; visualization, R.L.; writing—original draft, Y.Y., X.Z. and R.L.; writing—review and editing, T.M. All authors have read and agreed to the published version of the manuscript.

Funding: This research was funded by the Anhui Provincial Key Research and Development Project (grant number 202104a07020005), the University Synergy Innovation Program of Anhui Province (grant number GXXT-2022-019), and the State Key Laboratory of Mining Response and Disaster Prevention and Control in Deep Coal Mines Open Fund (grant number SKLMRDPC22KF20).

Institutional Review Board Statement: Not applicable.

Informed Consent Statement: Not applicable.

Data Availability Statement: The data presented in this study are available on request from the authors.

Conflicts of Interest: The authors declare no conflict of interest.

References

1. Yan, W.; Ya-ru, Z.; Yong, M. Study on the coal mine personnel position system based on wireless body sensor networks. In Proceedings of the 2008 5th International Summer School and Symposium on Medical Devices and Biosensors, Hong Kong, China, 1–3 June 2008; pp. 75–78.
2. Duta, N. A survey of biometric technology based on hand shape. *Pattern Recognit.* **2009**, *42*, 2797–2806. [CrossRef]
3. Malaspina, D.; Coleman, E.; Goetz, R.R.; Harkavy-Friedman, J.; Corcoran, C.; Amador, X.; Yale, S.; Gorman, J.M. Odor identification, eye tracking and deficit syndrome schizophrenia. *Biol. Psychiatry* **2002**, *51*, 809–815. [CrossRef]
4. Park, H.A.; Park, K.R. Iris recognition based on score level fusion by using SVM. *Pattern Recognit. Lett.* **2007**, *28*, 2019–2028. [CrossRef]
5. Kurita, K. Human identification from walking signal based on measurement of current generated by electrostatic induction. *Kansei Eng. Int. J.* **2012**, *11*, 183–189. [CrossRef]
6. Little, J.; Boyd, J. Recognizing people by their gait: The shape of motion. *Videre J. Comput. Vis. Res.* **1998**, *1*, 1–32.
7. Nickel, C.; Busch, C.; Rangarajan, S.; Möbius, M. Using hidden markov models for accelerometer-based biometric gait recognition. In Proceedings of the 2011 IEEE 7th International Colloquium on Signal Processing and its Applications, Penang, Malaysia, 4–6 March 2011; pp. 58–63.
8. Wu, Z.; Huang, Y.; Wang, L.; Wang, X.; Tan, T. A comprehensive study on cross-view gait based human identification with deep cnns. *IEEE Trans. Pattern Anal. Mach. Intell.* **2016**, *39*, 209–226. [CrossRef] [PubMed]
9. Konz, L.; Hill, A.; Banaei-Kashani, F. ST-DeepGait: A Spatiotemporal Deep Learning Model for Human Gait Recognition. *Sensors* **2022**, *22*, 8075. [CrossRef] [PubMed]
10. Zhang, Y.; Pan, G.; Jia, K.; Lu, M.; Wang, Y.; Wu, Z. Accelerometer-based gait recognition by sparse representation of signature points with clusters. *IEEE Trans. Cybern.* **2014**, *45*, 1864–1875. [CrossRef] [PubMed]
11. Al-Naimi, I.; Wong, C.B.; Moore, P.; Chen, X. Multimodal approach for non-tagged indoor identification and tracking using smart floor and pyroelectric infrared sensors. *Int. J. Comput. Sci. Eng.* **2017**, *14*, 1–15.
12. Augustin, A.; Yi, J.; Clausen, T.; Townsley, W.M. A study of LoRa: Long range & low power networks for the internet of things. *Sensors* **2016**, *16*, 1466. [PubMed]
13. Peng, Y.; Shangguan, L.; Hu, Y.; Qian, Y.; Lin, X.; Chen, X.; Fang, D.; Jamieson, K. PLoRa: A passive long-range data network from ambient LoRa transmissions. In Proceedings of the 2018 Conference of the ACM Special Interest Group on Data Communication, Budapest, Hungary, 20–25 August 2018; pp. 147–160.
14. Berni, A.; Gregg, W. On the utility of chirp modulation for digital signaling. *IEEE Trans. Commun.* **1973**, *21*, 748–751. [CrossRef]
15. Jennison, B.K. Performance of a linear frequency-modulated signal detection algorithm. In Proceedings of the Record of the IEEE 2000 International Radar Conference [Cat. No. 00CH37037], Alexandria, VA, USA, 7–12 May 2000; pp. 447–450.
16. Zhu, R.; Zhou, Z. A real-time articulated human motion tracking using tri-axis inertial/magnetic sensors package. *IEEE Trans. Neural Syst. Rehabil. Eng.* **2004**, *12*, 295–302. [PubMed]
17. Glowinski, S.; Blazejewski, A.; Krzyzynski, T. Human gait feature detection using inertial sensors wavelets. In Proceedings of the Wearable Robotics: Challenges and Trends: Proceedings of the 2nd International Symposium on Wearable Robotics, WeRob2016, Segovia, Spain, 18–21 October 2016; Springer: Berlin/Heidelberg, Germany, 2017; pp. 397–401.
18. Tadano, S.; Takeda, R.; Miyagawa, H. Three dimensional gait analysis using wearable acceleration and gyro sensors based on quaternion calculations. *Sensors* **2013**, *13*, 9321–9343. [CrossRef] [PubMed]
19. Liu, X.; Liu, J. Gait recognition method of underground coal mine personnel based on densely connected convolution network and stacked convolutional autoencoder. *Entropy* **2020**, *22*, 695. [CrossRef] [PubMed]
20. Chao, L.; Jinye, P.; Wang, Z.; Shi, Y. Gait Recognition Underground Coal Mine by Combining Wavelet Packet Transforms and Principle Component Analysis. In Proceedings of the 2015 Sixth International Conference on Intelligent Systems Design and Engineering Applications (ISDEA), Guizhou, China, 18–19 August 2015; pp. 421–425.
21. Li, X.; Wang, S.; Liu, B.; Chen, W.; Fan, W.; Tian, Z. Improved YOLOv4 network using infrared images for personnel detection in coal mines. *J. Electron. Imaging* **2022**, *31*, 013017. [CrossRef]
22. Shi, C.; Liu, J.; Liu, H.; Chen, Y. Smart user authentication through actuation of daily activities leveraging WiFi-enabled IoT. In Proceedings of the 18th ACM International Symposium on Mobile Ad Hoc Networking and Computing, Chennai, India, 10–14 July 2017; pp. 1–10.
23. Wang, W.; Liu, A.X.; Shahzad, M. Gait recognition using wifi signals. In Proceedings of the 2016 ACM International Joint Conference on Pervasive and Ubiquitous Computing, Heidelberg, Germany, 12–16 September 2016; pp. 363–373.
24. Zeng, Y.; Pathak, P.H.; Mohapatra, P. WiWho: WiFi-based person identification in smart spaces. In Proceedings of the 2016 15th ACM/IEEE International Conference on Information Processing in Sensor Networks (IPSN), Vienna, Austria, 11–14 April 2016; pp. 1–12.
25. Zhang, J.; Wei, B.; Hu, W.; Kanhere, S.S. Wifi-id: Human identification using wifi signal. In Proceedings of the 2016 International Conference on Distributed Computing in Sensor Systems (DCOSS), Washington, DC, USA, 26–28 May 2016; pp. 75–82.
26. Xin, T.; Guo, B.; Wang, Z.; Li, M.; Yu, Z.; Zhou, X. Freesense: Indoor human identification with Wi-Fi signals. In Proceedings of the 2016 IEEE Global Communications Conference (GLOBECOM), Washington, DC, USA, 4–8 December 2016; pp. 1–7.
27. Vandersmissen, B.; Knudde, N.; Jalalvand, A.; Couckuyt, I.; Bourdoux, A.; De Neve, W.; Dhaene, T. Indoor person identification using a low-power FMCW radar. *IEEE Trans. Geosci. Remote Sens.* **2018**, *56*, 3941–3952. [CrossRef]

28. Zhao, P.; Lu, C.X.; Wang, J.; Chen, C.; Wang, W.; Trigoni, N.; Markham, A. mid: Tracking and identifying people with millimeter wave radar. In Proceedings of the 2019 15th International Conference on Distributed Computing in Sensor Systems (DCOSS), Santorini Island, Greece, 29–31 May 2019; pp. 33–40.
29. Meng, Z.; Fu, S.; Yan, J.; Liang, H.; Zhou, A.; Zhu, S.; Ma, H.; Liu, J.; Yang, N. Gait recognition for co-existing multiple people using millimeter wave sensing. In Proceedings of the AAAI Conference on Artificial Intelligence, New York, NY, USA, 7–12 February 2020; Volume 34, pp. 849–856.
30. Li, T.; Cao, X.; Liu, H.; Shi, C.; Chen, P. MTPGait: Multi-person Gait Recognition with Spatio-temporal Information via Millimeter Wave Radar. In Proceedings of the 2021 IEEE 27th International Conference on Parallel and Distributed Systems (ICPADS), Beijing, China, 14–16 December 2021; pp. 660–666.
31. Hossain, T.; Doi, Y.; Tazin, T.; Ahad, M.A.R.; Inoue, S. Study of lorawan technology for activity recognition. In Proceedings of the 2018 ACM International Joint Conference and 2018 International Symposium on Pervasive and Ubiquitous Computing and Wearable Computers, Singapore, 8–12 October 2018; pp. 1449–1453.
32. Petäjäjärvi, J.; Mikhaylov, K.; Yasmin, R.; Hämäläinen, M.; Iinatti, J. Evaluation of LoRa LPWAN technology for indoor remote health and wellbeing monitoring. *Int. J. Wirel. Inf. Netw.* **2017**, *24*, 153–165. [CrossRef]
33. Ke, K.H.; Liang, Q.W.; Zeng, G.J.; Lin, J.H.; Lee, H.C. A LoRa wireless mesh networking module for campus-scale monitoring: demo abstract. In Proceedings of the 6th ACM/IEEE International Conference on Information Processing in Sensor Networks, Milano, Italy, 4–6 May 2017; pp. 259–260.
34. Chen, L.; Xiong, J.; Chen, X.; Lee, S.I.; Chen, K.; Han, D.; Fang, D.; Tang, Z.; Wang, Z. WideSee: Towards wide-area contactless wireless sensing. In Proceedings of the 17th Conference on Embedded Networked Sensor Systems, New York, NY, USA, 10–13 November 2019; pp. 258–270.
35. Zhang, F.; Chang, Z.; Niu, K.; Xiong, J.; Jin, B.; Lv, Q.; Zhang, D. Exploring lora for long-range through-wall sensing. *Proc. ACM Interact. Mobile Wearable Ubiquitous Technol.* **2020**, *4*, 68. [CrossRef]
36. Zhang, F.; Chang, Z.; Xiong, J.; Zheng, R.; Ma, J.; Niu, K.; Jin, B.; Zhang, D. Unlocking the beamforming potential of LoRa for long-range multi-target respiration sensing. *Proc. ACM Interact. Mobile Wearable Ubiquitous Technol.* **2021**, *5*, 85. [CrossRef]
37. Xie, B.; Xiong, J. Combating interference for long range LoRa sensing. In Proceedings of the 18th Conference on Embedded Networked Sensor Systems, Virtual, 16–19 November 2020; pp. 69–81.

Disclaimer/Publisher's Note: The statements, opinions and data contained in all publications are solely those of the individual author(s) and contributor(s) and not of MDPI and/or the editor(s). MDPI and/or the editor(s) disclaim responsibility for any injury to people or property resulting from any ideas, methods, instructions or products referred to in the content.